Ferroelectric Properties of Perovskite Thin Films and Their Implications for Solar Energy Conversion

*Holger Röhm, Tobias Leonhard, Alexander D. Schulz, Susanne Wagner, Michael J. Hoffmann, and Alexander Colsmann**

Whether or not methylammonium lead iodide ($MAPbI_3$) is a ferroelectric semiconductor has caused controversy in the literature, fueled by many misunderstandings and imprecise definitions. Correlating recent literature reports and generic crystal properties with the authors' experimental evidence, the authors show that $MAPbI_3$ thin-films are indeed semiconducting ferroelectrics and exhibit spontaneous polarization upon transition from the cubic high-temperature phase to the tetragonal phase at room temperature. The polarization is predominantly oriented in-plane and is organized in characteristic domains as probed with piezoresponse force microscopy. Drift-diffusion simulations based on experimental patterns of polarized domains indicate a reduction of the Shockley–Read–Hall recombination of charge carriers within the perovskite grains due to the ferroelectric built-in field and allow reproduction of the electrical solar cell properties.

1. Introduction

Efficient charge carrier separation and transport in organic metal halide (OMH) perovskites have enabled a new class of solar cells.[1] Even rather simple device architectures comprising polycrystalline light-harvesting OMH layers processed from solution can exhibit high power conversion efficiencies.

H. Röhm, T. Leonhard, A. D. Schulz, Dr. A. Colsmann
Karlsruhe Institute of Technology
Light Technology Institute (LTI)
Engesserstrasse 13, 76131 Karlsruhe, Germany
E-mail: alexander.colsmann@kit.edu
H. Röhm, T. Leonhard, A. D. Schulz, Prof. M. J. Hoffmann,
Dr. A. Colsmann
Karlsruhe Institute of Technology
Material Research Center for Energy Systems (MZE)
Strasse am Forum 7, 76131 Karlsruhe, Germany
Dr. S. Wagner, Prof. M. J. Hoffmann
Karlsruhe Institute of Technology
Institute for Applied Materials – Ceramic Materials and Technologies (IAM)
Haid-und-Neu-Strasse 7, 76131 Karlsruhe, Germany

The ORCID identification number(s) for the author(s) of this article can be found under https://doi.org/10.1002/adma.201806661.

Yet, as of today, the microscopic origin of the remarkable charge carrier dynamics in perovskite solar cells remains unclear. An often proposed idea to explain the enhanced separation and transport of photogenerated charge carriers describes the formation of ferroelectric domains, i.e., domains with alternating polarization. Ferroelectric domains would provide local internal electric fields that assist with the separation of charge carriers and hence reduce recombination.[2–4] However, whether or not OMH perovskites are ferroelectric materials or exhibit other ferroic properties, and which effects might result from these properties have been a subject of debate for several years. A multitude of measurement techniques was employed in order to probe ferroic properties of single crystal samples,[5,6] pressed powder pellets,[7] and polycrystalline thin-films[8] of OMH perovskites. Scanning microscopy techniques such as atomic force microscopy (AFM),[9–12] scanning electron microscopy (SEM),[13] and tunneling electron microscopy (TEM)[14] were extensively used in order to reveal the microstructure of OMH-perovskite thin-film samples with subgrain resolution. Some of these studies revealed ordered domains within crystal grains, but no consensus has been reached about the interpretation of their ferroic and crystallographic origins. Claims included piezo-electricity,[15–17] pyroelectricity,[5] ferroelasticity,[9,12,18] anti-ferroelectricity[19] as well as ferroelectricity,[10,11,15,16,20] and the seemingly contradictory reports on these ferroic properties have heated up the discussion. Techniques that probe large areas of specimens such as X-ray diffraction (XRD),[21] imped-ance spectroscopy,[22,23] and J–V characterization[5,7] added a rather spatially averaged picture of the samples' microstructure. For example, second harmonic generation (SHG) measurements were employed in order to identify whether or not OMH perovskites form polar crystals, but their interpretation led to ambiguous results.[5,24]

In order to clarify some of the confusion and seemingly contradictory reports on the ferroic and, in particular, ferroelectric features of OMH perovskites, we review and discuss some of the fundamental properties of this material class and correlate them with our own observations on perovskite thin-films. We deliberately focus on the ferroic properties of archetypical methylammonium lead iodide ($MAPbI_3$), representing the class of light-harvesting perovskites.
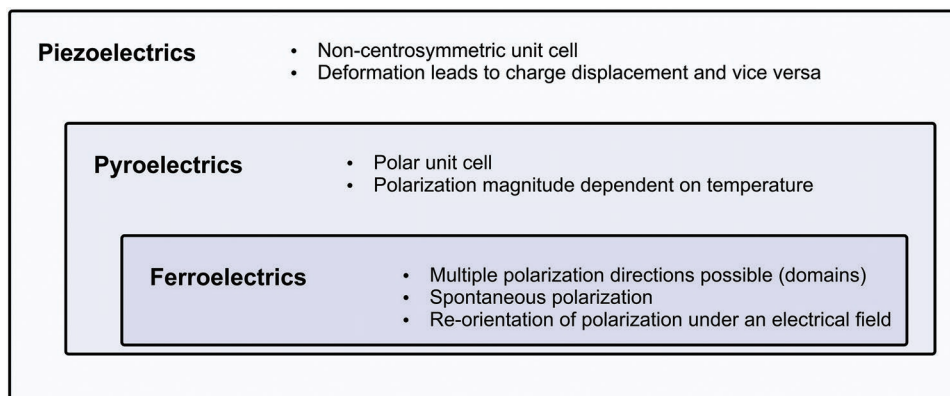
**ADVANCED
SCIENCE NEWS**
www.advancedsciencenews.com

**ADVANCED
MATERIALS**
www.advmat.de

Figure 1. Diagram of the non-centrosymmetric crystal classes and their ferroic properties.

2. Ferroic Properties

To begin with, we want to review the various electric ferroic properties that generic crystalline materials can have. We deliberately exclude any magnetic ferroic material properties from our discussion as these have not been reported in MAPbI$_3$ in the literature to date. The ferroic properties of a crystal are determined by the structure and symmetry of its unit cell. Any break of the symmetry can incur a responsivity of the crystal to external stimuli. Therefore, all ferroic materials are non-centrosymmetric. **Figure 1** shows a schematic overview of the ferroic crystal classes.

2.1. Piezoelectrics

In 20 of the total 21 non-centrosymmetric crystal classes, deformation leads to a displacement of charges and vice versa. These piezoelectrics can be probed by applying an external mechanical stress and measuring the resulting voltage at opposite crystal faces (piezoelectric effect), or by applying an electrical field and measuring the resulting deformation of the crystal (inverse or converse piezoelectric effect). Piezoelectricity can be probed with high spatial resolution by piezoresponse force microscopy (PFM). In this AFM technique, a modulated electrical field between a conductive tip and the sample generates a coherent mechanical response detectable by the deflection of the cantilever.

2.2. Pyroelectrics

Among the 20 piezoelectric crystal classes, 10 exhibit permanently polarized unit cells. These crystal classes are referred to as pyroelectrics. The built-in dipole leads to a strong electrical field in pyroelectric crystals, which is compensated by accumulation of charge carriers at the crystal surfaces. The magnitude of polarization in pyroelectrics depends on the temperature. Upon cooling or heating, the equilibrium of crystal polarization and compensating surface charges is temporarily shifted. This shift of the equilibrium induces a potential difference at the crystal faces, which is then compensated by a flow of charges. The higher the electrical or ionic conductivity of the crystal is, the faster this compensation takes place. Pyroelectricity is probed by measuring the surface potential difference and the corresponding compensation currents while heating or cooling a crystal at a constant rate. All pyroelectrics are also piezoelectric.

2.3. Ferroelectrics

In a subset of pyroelectrics, the so-called ferroelectrics, the spontaneous polarization of each unit cell can be reoriented under a sufficiently strong external electrical bias. The resulting polarization hysteresis is well known from poling experiments on insulating ferroelectric perovskites, such as barium titanate (BaTiO$_3$) or lead zirconate titanate (PZT),[25] and is the classical hallmark of ferroelectrics.[26] This polarizability of ferroelectrics can also become visible without applying an external field: when the crystal cools from the paraelectric (non-ferroelectric) to the ferroelectric phase, polarized domains comprising unit cells with parallel dipole orientation can form spontaneously which is also often considered as the definition and a fail-proof signature of ferroelectrics.[27] The temperature of phase transition from the ferroelectric to the paraelectric phase or vice versa is referred to as the Curie temperature T_c. For example, a phase transition from a cubic crystal structure (above T_c) to a tetragonal crystal structure (below T_c) leads to mechanical stress, to a break of centrosymmetry, to a spontaneous polarization of the unit cell and hence to electrical fields in a crystal, which are partially compensated by charge carrier accumulations that generate depolarizing fields. This can lead to the formation of domains with alternating polarization in order to minimize the free energy. After this relaxation process, mediated by domain formation, a ferroelectric crystal typically has zero macroscopic net polarization and zero residual strain.[28] The existence of multiple polarized domains within a crystal is a unique feature of ferroelectrics. All ferroelectrics are piezoelectric and pyroelectric.

2.4. Anti-Ferroelectrics

Ferroelectric domains with alternating polarization are sometimes confused with anti-ferroelectric crystal properties. Anti-ferroelectrics exhibit an energetically favorable, antiparallel alignment of neighboring unit cells such that the polarization
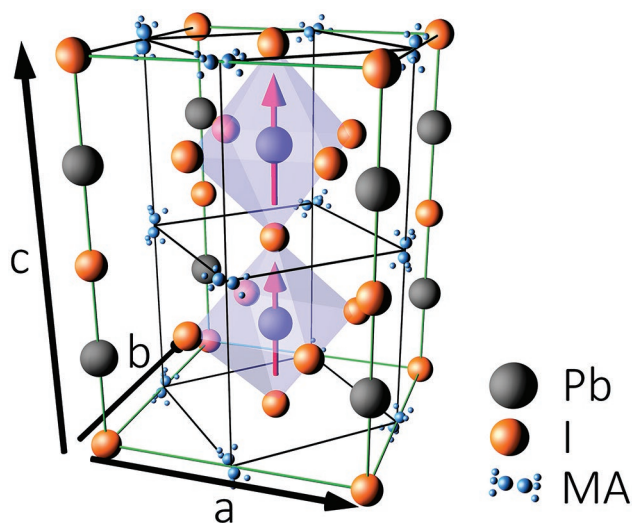
**ADVANCED
SCIENCE NEWS**
www.advancedsciencenews.com

**ADVANCED
MATERIALS**
www.advmat.de

Figure 2. Schematic representation of the tetragonal unit cell of MAPbI$_3$ at room temperature (green frame). Red arrows indicate the polarization of the unit cell along the *c*-axis. The pseudocubic perovskite lattice is indicated by black frames.

of neighboring unit cells is compensated. An anti-ferroelectric crystal cannot form stable domains over multiple unit cells. Upon application of a sufficiently strong external electric field, the polarization orientation of the unit cells in an anti-ferroelectric crystal can be temporarily aligned in one direction, but the crystal immediately reverts to its initial state when the external electric field is switched off (no remanent polarization).

2.5. Ferroelastics

Ferroelastics are not part of the crystal hierarchy that is depicted in **Figure 2**, but rather describe materials with certain mechanical properties: Sufficiently high mechanical stress can lead to deformation and a change of the crystal orientation or crystal phase. This ferroelastic switching can mediate the formation of twin domains of alternating crystal phases or orientation. Purely ferroelastic domains are mechanical in nature, do not possess electrical dipoles, and hence are not influenced by external electrical fields. Ferroelasticity can be considered the mechanical equivalent to ferroelectricity. Ferroelastic domains can be probed via measurement techniques that reveal the local crystal structure in each domain (e.g., via TEM or μ-beam XRD) or by observation of topographical features of twinned domains at the crystal surface (e.g., via AFM or SEM).[29] Notably, while not all ferroelastic materials are ferroelectric, all common ferroelectric materials are also ferroelastic. This is why the formation of ferroelectric domains can very well be influenced by the mechanical stress that occurs when the crystal cools down below T_c.

3. Experimental Evidence of Ferroelectric Domains in MAPbI$_3$ Thin-films

MAPbI$_3$ can exhibit orthorhombic ($Pna2_1$), tetragonal ($I4cm$), or cubic ($Pm3m$) crystal phases depending on the

temperature.[30,31] The orthorhombic and tetragonal phases are non-centrosymmetric, piezoelectric space groups, whereas the cubic phase is centrosymmetric. For solar cell applications, only the tetragonal phase of MAPbI$_3$ at room temperature and the cubic high-temperature phase above 327 K are relevant. Figure 2 illustrates the crystal structure of MAPbI$_3$ in its tetragonal phase at room temperature. The MAPbI$_3$ unit cell comprises two perovskite cubes with slightly twisted PbI$_6$ octahedrons (purple).[31] The pseudocubic perovskite lattice is 0.5% strained along the *c*-axis which imposes the tetragonal crystal structure onto MAPbI$_3$. We note that the coexistence of tetragonal and cubic crystal phases up to 350 K has been reported.[32]

With the mandatory requirements of non-centrosymmetry and piezoelectricity of the crystal structure being fulfilled, the question remains if any experimental evidence of ferroelectricity in MAPbI$_3$ in its tetragonal phase at room temperature exists. While most ceramic ferroelectrics are insulators that allow for evidencing ferroelectricity by electrical switching of the polarization without significant leakage currents, OMH perovskites are semiconductors. Therefore, switching cannot readily be accomplished by applying a high DC voltage. Electrical fields stronger than ≈4 V μm^{-1} lead to high electrical currents through the semiconductor and hence may thermally destroy the perovskite layer. Rakita et al. succeeded in poling tetragonal MAPbI$_3$ crystals under an electrical bias by lowering the temperature to 204 K, thus reducing the charge carrier mobility and the leakage current.[5] In addition, under an external electric poling field, the high ionic conductivity of iodide in MAPbI$_3$ may superimpose electrical effects or change the local material composition.[33] This is why, to date, poling experiments are not a reliable tool to prove or disprove ferroelectricity in semiconducting perovskites such as MAPbI$_3$, and why the observation of domain formation by spontaneous polarization is the only reliable evidence of their ferroelectricity.

Typical perovskite solar cells comprise polycrystalline thin-films with thicknesses of a few hundred nanometers. Macroscopic measurements of the thin-film properties only show superimposed effects from many grains. Therefore, the investigation of the microstructure and possible ferroelectric properties of perovskite thin-films requires measurement techniques with smaller-than-grain-diameter resolution (100–1000 nm) such as AFM, PFM, or Kelvin probe force microscopy (KPFM). We note that the dimensions of the grains influence the ferroic features, such as the width and orientation of domains, which may partly account for different data interpretations throughout the literature.[34] In contrast to large single crystal samples, the properties of grains in thin-films are strongly influenced by interfaces, which are relatively large with respect to the crystal volume. Therefore, changing the substrate and interface beneath the perovskite layer does influence its grain growth and microstructure.[10] In addition, every process parameter that influences crystallization, such as annealing temperature and duration, could influence the orientation and size of grains and thereby any ferroic properties.

Figure 3a depicts the topography of a representative MAPbI$_3$ perovskite thin-film sample on top of a glass/indium tin oxide (ITO)/poly(3,4-ethylenedioxythiophene):polystyrene sulfonate (PEDOT:PSS) substrate as measured by AFM, revealing
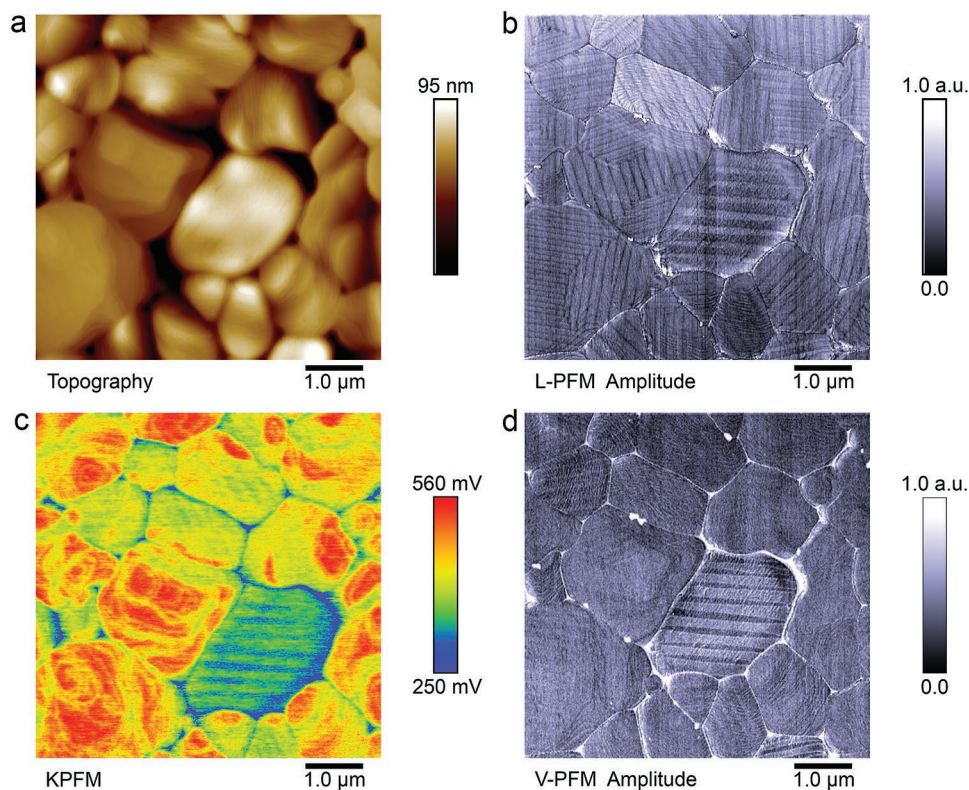
ADVANCED
SCIENCE NEWS
www.advancedsciencenews.com

ADVANCED
MATERIALS
www.advmat.de

Figure 3. a) Topography, b) L-PFM, c) KPFM, and d) V-PFM maps of the same MAPbI$_3$ thin-film sample. The large flat grains reveal domains of alternating, predominantly in-plane polarization. In the KPFM measurement, most grain surfaces exhibit similar work functions without significant influence from the domains that are visible in PFM images. Yet, one grain exhibits exactly the same domain pattern in KPFM and PFM imaging, revealing domain-driven surface polarization. (Scanning rate: 0.5 Hz in all measurements, PFM scanning angle: 90°, KPFM scanning angle: 0°. $f_{L\text{-}PFM}$ = 60.4 kHz, $f_{V\text{-}PFM}$ = 191.6 kHz.)

flat grains with typical diameters of 1–3 µm. The very same deposition process yields highly efficient perovskite solar cells with power conversion efficiencies of up to 16% (glass/ITO/PEDOT:PSS/MAPbI$_3$/[6,6]-phenyl C$_{71}$-butyric acid methyl ester (PC[71]BM)/bathocuproine (BCP)/Ag, fabricated in nitrogen atmosphere).[10] The large, flat, and featureless grains were fabricated by sample annealing above T_c (T = 100 °C, 60 min) and subsequent cooling to room temperature. This sample geometry minimizes any crosstalk from topography to other scanning probe measurements. Importantly, the micrographs depicted in Figure 3 were recorded in a glovebox under nitrogen atmosphere, so that the samples have never been exposed to air, in order to prevent contamination and deterioration of the sample surface.

Due to the non-centrosymmetry of the tetragonal unit cell at room temperature, MAPbI$_3$ thin-films exhibit piezoresponsivity which allows monitoring their properties using single-frequency PFM (sf-PFM). The PFM signal is obtained by applying an alternating electrical field between the bottom electrode of the sample and the AFM tip and by correlating this stimulus with the local mechanical response (inverse piezoelectric effect) of the MAPbI$_3$ layer. By measuring lateral (torsion of the cantilever) or vertical (deflection) movements of the AFM tip near the respective resonance frequencies, lateral (in-plane, L-PFM) and vertical (out-of-plane, V-PFM) crystal responses can further be distinguished. We note that sf-PFM measurements near the resonance frequency are sometimes

susceptible to misinterpretation. However, Vorpahl et al. have demonstrated that dual-resonance tracking PFM obtains similar results to sf-PFM data.[11] Figure 3b shows the L-PFM image of the same sample position. Not only do we see a clear piezoresponse of the sample, but also do we observe 90 nm wide parallel stripes where the topography is absolutely featureless. The corresponding L-PFM phase images typically show a distinct 180° phase contrast between stripes.[21] Therefore, these stripes represent crystal domains of alternating polarization. As depicted in Figure 3d, on the vast majority of grains, these domains are hardly visible in V-PFM which lets us conclude that the direction of polarization in these grains is oriented in-plane.[21] The weak domain pattern in V-PFM may stem from a vertical deflection of the scanning cantilever by the lateral deformation of the crystal (buckling effects). We note that contact-resonance enhanced PFM measurements do not yield absolute magnitudes of polarization, but the strong contrast between domains on each grain unambiguously demonstrates varying mechanical response to the electrical stimulus in each domain region. The previously reported appearance of such domains in transmission electron micrographs provides evidences that the domains are a bulk property rather than a surface effect.[14] The existence of piezoresponsive alternating domains in these MAPbI$_3$ grains cannot be explained with a purely piezoelectric or pyroelectric crystal. The formation of alternating polar domains is a unique feature of ferroelectric materials. Purely ferroelastic (non-ferroelectric) twin domains

would not respond to an electrical stimulus. However, we note that the formation of domains can be influenced by mechanical stress since every common ferroelectric material is also ferroelastic (see definitions above). This subtlety may well have contributed to the confusion and heated discussions around the ferroelectricity and/or ferroelasticity of MAPbI$_3$ in the past. Likewise, reports in the literature attempted to explain the PFM data of MAPbI$_3$ thin-films with ionic charging of the sample surface or areas of varying chemistry or phase.[12,35] While ions certainly play an important role in the understanding of MAPbI$_3$, the differences between L-PFM and V-PFM data as shown in Figure 3b,d exclude surface effects such as ionic charge accumulation to be the origin of the PFM signal.[36,37] While the polarization of domains can lead to charge carrier accumulation at surfaces,[38] such surface effects by themselves could not lead to the sharp contrast between neighboring domains with in-plane polarization and 180° phase contrasts. Likewise, electrostriction would only affect V-PFM measurements and not L-PFM measurements and, therefore, can also be excluded as the origin for domain contrast. Taking all the known literature data to date and our own measurements into account, we conclude that MAPbI$_3$ thin-films are semiconducting ferroelectrics.

While the vast majority of grains exhibit strong in-plane polarization (L-PFM, Figure 3b) and, at most, only weak out-of-plane polarization, occasionally, individual grains with both in-plane and out-of-plane polarization components were observed.[21] At the same time, their domain patterns can have different shapes than the strictly 90 nm wide stripes. A typical example is the grain in the center of the micrographs in Figure 3. Since the polarization of the unit cell is correlated with its *c*-axis,[5] the different polarization pattern indicates a different crystal orientation than the surrounding grains.[21] Different crystal orientations and concurrently different crystal faces, however, would become visible in measurements of the surface potential. Indeed, the KPFM image in Figure 3c reveals a surface potential of about 500 mV (relative to AFM tip, red/orange) on most grains, except for the one grain in the center of the image that produces the different polarization patterns. This grain exhibits significantly lower surface potential (≈300 mV, blue/green). In addition, the pattern of the polar domains is superimposed on the low surface potential of this grain. This finding suggests that the out-of-plane component of the alternating polarization on the differently oriented grain also modulates the surface potential.

The PFM measurements enable conclusions on the in-plane polarization of the MAPbI$_3$ thin-films, but the in-plane direction of the polarization vector remains hidden. Yet, symmetry considerations on the domain assembly allow for some conclusions. As exemplified in **Figure 4**, occasionally, domains and domain walls were observed that continue at an angle of about 90°.[10] For reasons of symmetry, we conclude that these domains exhibit a polarization that is oriented 45° relative to the domain walls. Any other orientation would create two regimes of different polarization within one 90°-continuing domain. Furthermore, the contrast of amplitude between neighboring domains in L-PFM excludes 180° domain walls (antiparallel polarization direction), which would exclusively differ in the phase of the PFM signal. For the majority of grains with in-plane polarization, these considerations
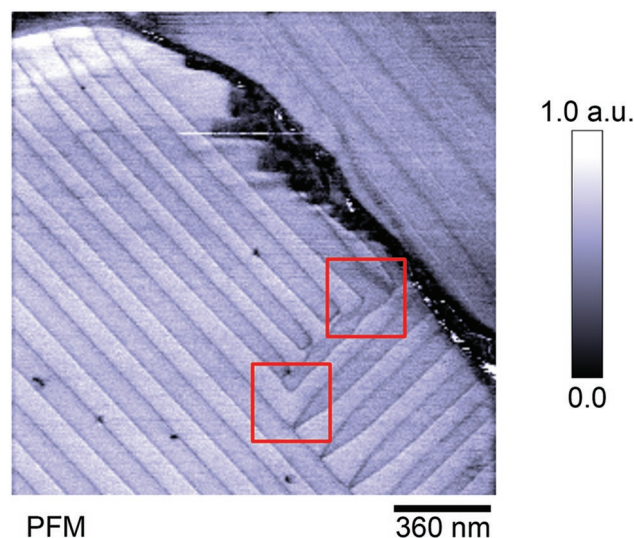

Figure 4. High-resolution PFM image of polar domains on a MAPbI$_3$ grain. Occasionally, domains continue at angles of 90° (marked with red squares) within the same grain. Adapted by permission.[10] Copyright 2017, The Royal Society of Chemistry.

leave two possible domain configurations: the polarization direction in neighboring domains can either be organized head-to-head which would create charged domain walls, or head-to-tail which would leave the domain walls uncharged. In both cases, the polarization directions of neighboring domains form a 90° angle and a 45° angle with the domain walls.

While the PFM measurements provide a clear picture about the polarization of MAPbI$_3$ thin-films, the origin of the polarization in MAPbI$_3$ remains to be investigated. Well-known ferroelectrics such as BaTiO$_3$ exhibit spontaneous polarization upon cooling below T_c by displacement of atoms along the *c*-axis, breaking the centrosymmetry and generating a polar axis. Indeed, in common inorganic ferroelectric perovskites, typically, the B-site cation is displaced, producing a polarization of the unit cell.[39,40] In MAPbI$_3$, this would correspond to a displacement of the Pb atom, but the experimental evidence is yet to be produced. Other previous works proposed that the dipolar methylammonium aligns in the crystal cage and thus produces polar unit cells.[2] At the same time, some simulations predicted that the methylammonium freely rotates within the crystal cage which would translate into no contribution to the polarization of the material.[41] Gallop et al. reported a preferentially oriented tumbling of the molecule[42] and Tan et al. concluded that the dipole orientation correlates with distortion of the tetragonal crystal lattice.[43] Whether or not the organic molecule plays a role for the polarization in MAPbI$_3$ could be further explored in the future by changing the dipolar momentum of the A-site cation, e.g., by using nondipolar molecules or single atoms, and by tracking the changes in the polarization.

4. Implications for Material Design

The discussion surrounding the existence or absence of ferroelectric polar domains is mainly driven by which kind
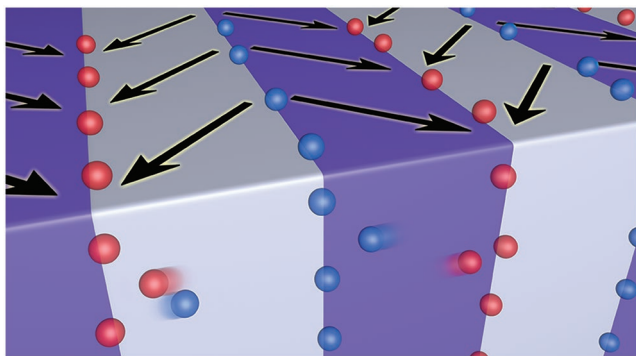
Figure 5. Schematic representation of a typical ferroelectric domain configuration in a MAPbI$_3$ thin-film with charged domain walls (head-to-head and tail-to-tail domain polarization). The built-in electrical field drives electrons and holes apart toward different domain walls which, according to simulations, reduce the overall charge carrier recombination rate.

of influence such domains may have on the thin-film properties and ultimately the solar cell performance. This is pivotally important, not only for optimizing existing OMH perovskites, but in particular as a design criterion for new, more stable, and eco-friendly light-harvesting perovskites. Early simulations predicted a positive influence of polar domains on solar cell properties by generating separate charge carrier pathways that are energetically favorable for electrons or holes, thus reducing charge carrier recombination losses.[2–4]

While the experimental results reviewed here prove the existence of ferroelectricity in semiconducting MAPbI$_3$ thin-films, experimental evidence for an effect of the polar domains on the charge carrier recombination has not been achieved yet.

In order to understand how charge carriers in an illuminated MAPbI$_3$ thin-film are influenced by polarized domains, Rossi et al. conducted drift-diffusion simulations on experimentally observed domain patterns.[44] Assuming head-to-head and tail-to-tail orientation of the domain polarization, these simulations revealed that polarized domains in MAPbI$_3$ thin-films can effectively influence charge carriers, form separate electron- and hole-pathways and hence create charged domain walls as illustrated in **Figure 5**. This configuration reduces the Shockley–Read–Hall recombination losses within grains and improves the fill factor as well as the overall power conversion efficiency of the corresponding solar cells. The experimental current density–voltage (J–V) curves were best reproduced with a polarization strength of 0.2 µC cm^{-2}. While the experimental data described above allows for both charged and uncharged domain wall configurations, simulations cannot reproduce the J–V curves assuming uncharged domain walls (head-to-tail domain polarization). Uncharged domain walls would hardly influence the charge carrier recombination but in effect rather compare to a zero-polarization (non-ferroelectric) scenario. Although uncharged domain walls may exist in MAPbI$_3$ grains in a polycrystalline thin-film, better device performance will be achieved if their formation is suppressed. Importantly, vertical (out-of-plane) components of the polarization do not show any notable influence on charge carrier density or recombination rates since, in steady-state, these polarization components are compensated by charge carrier accumulation at the interfaces to anode and cathode, respectively. However, if nonohmic

contacts are assumed, the surface dipoles of vertically polarized domains may assist or hinder charge carrier extraction to the electrodes.[10,45] As described above, grains that exhibit such vertical polarization components were only observed occasionally in our experiments while the vast majority of grains showed in-plane polarization. In this light, the control of in-plane polarization deems to be important for future device and process designs. Yet, it remains to be investigated how to best control the polarization orientation in MAPbI$_3$ domains. Following up on recent discussions about ion migration in domains, we further speculate that, in dark conditions, charged domain walls are populated by ionic charge carriers (I$^-$, CH$_3$NH$_3^+$) that are gradually replaced by electrons and holes upon illumination. This process might contribute to changes in photocurrent during dynamic illumination.[46]

5. Conclusion and Perspective

MAPbI$_3$ thin-films are ferroelectric semiconductors. Any attempts to describe the experimental data with purely ferroelastic material properties, ionic charging, or ion migration assuming zero polarization (non-ferroelectricity), to date, remain incomplete.

MAPbI$_3$ thin-films can spontaneously form polar domains when samples cool down below T_c. Annealing and cooling from the nonpolar cubic phase to the tetragonal ferroelectric phase is a part of nearly all fabrication processes published by perovskite solar cell researchers in recent years which is why we expect the formation of ferroelectric domains to be a prevalent effect on sufficiently large grains in most research labs.

Yet, we note that different samples, even from the same material, can exhibit different properties. For example, MAPbI$_3$ single crystals might exhibit different ferroic properties than polycrystalline thin-films since the latter are mostly dominated by surface and interface effects. And even thin-films of MAPbI$_3$ may possess different properties, for example, when deposited onto different surfaces.

Here we focused on the well-established MAPbI$_3$ in order to carve out a principal understanding of the ferroelectric effects in light-harvesting perovskites. Future investigations will show to what extent these findings can be reproduced on other light-harvesting perovskite compositions with enhanced efficiencies and robustness such as multication OMH compositions. On all accounts, the debate about ferroic properties of OMH perovskites is adding new important aspects of crystallographic understanding to the material design and the quest for new light-harvesting perovskites.

Acknowledgements

Conflict of Interest

The authors declare no conflict of interest.

Keywords

[1] Q. Lin, A. Armin, R. C. R. Nagiri, P. Meredith, *Nat. Photonics* **2015**, *9*, 106.

[2] J. M. Frost, K. T. Butler, F. Brivio, C. H. Hendon, M. van Schilfgaarde, A. Walsh, *Nano Lett.* **2014**, *14*, 2584.

[3] A. Pecchia, D. Gentilini, D. Rossi, M. Auf der Maur, A. Di Carlo, *Nano Lett.* **2016**, *16*, 988.

[4] A. M. A. Leguy, J. M. Frost, A. P. McMahon, V. G. Sakai, W. Kockelmann, C. Law, X. Li, F. Foglia, A. Walsh, B. C. O'Regan, J. Nelson, J. T. Cabral, P. R. F. Barnes, *Nat. Commun.* **2015**, *6*, 7124.

[5] Y. Rakita, O. Bar-Elli, E. Meirzadeh, H. Kaslasi, Y. Peleg, G. Hodes, I. Lubomirsky, D. Oron, D. Ehre, D. Cahen, *Proc. Natl. Acad. Sci. USA* **2017**, *114*, E5504.

[6] Q. Dong, Y. Fang, Y. Shao, P. Mulligan, J. Qiu, L. Cao, J. Huang, *Science* **2015**, *347*, 967.

[7] T.-Y. Yang, G. Gregori, N. Pellet, M. Grätzel, J. Maier, *Angew. Chem.* **2015**, *127*, 8016.

[8] M. Saliba, J.-P. Correa-Baena, M. Grätzel, A. Hagfeldt, A. Abate, *Angew. Chem.* **2018**, *130*, 2582.

[9] I. M. Hermes, S. A. Bretschneider, V. W. Bergmann, D. Li, A. Klasen, J. Mars, W. Tremel, F. Laquai, H.-J. Butt, M. Mezger, R. Berger, B. J. Rodriguez, S. A. L. Weber, *J. Phys. Chem. C* **2016**, *120*, 5724.

[10] H. Röhm, T. Leonhard, M. J. Hoffmann, A. Colsmann, *Energy Environ. Sci.* **2017**, *10*, 950.

[11] S. M. Vorpahl, R. Giridharagopal, G. E. Eperon, I. M. Hermes, S. A. L. Weber, D. S. Ginger, *ACS Appl. Energy Mater.* **2018**, *1*, 1534.

[12] Y. Liu, L. Collins, R. Proksch, S. Kim, B. R. Watson, B. Doughty, T. R. Calhoun, M. Ahmadi, A. V. Ievlev, S. Jesse, S. T. Retterer, A. Belianinov, K. Xiao, J. Huang, B. G. Sumpter, S. V. Kalinin, B. Hu, O. S. Ovchinnikova, *Nat. Mater.* **2018**, *17*, 1013.

[13] D. W. de Quilettes, S. M. Vorpahl, S. D. Stranks, H. Nagaoka, G. E. Eperon, M. E. Ziffer, H. J. Snaith, D. S. Ginger, *Science* **2015**, *348*, 683.

[14] M. U. Rothmann, W. Li, Y. Zhu, U. Bach, L. Spiccia, J. Etheridge, Y.-B. Cheng, *Nat. Commun.* **2017**, *8*, 14547.

[15] S. Ippili, V. Jella, J. Kim, S. Hong, S.-G. Yoon, *Nano Energy* **2018**, *49*, 247.

[16] Y.-J. Kim, T.-V. Dang, H.-J. Choi, B.-J. Park, J.-H. Eom, H.-A. Song, D. Seol, Y. Kim, S.-H. Shin, J. Nah, S.-G. Yoon, *J. Mater. Chem. A* **2016**, *4*, 756.

[17] Q. Dong, J. Song, Y. Fang, Y. Shao, S. Ducharme, J. Huang, *Adv. Mater.* **2016**, *28*, 2816.

[18] E. Strelcov, Q. Dong, T. Li, J. Chae, Y. Shao, Y. Deng, A. Gruverman, J. Huang, A. Centrone, *Sci. Adv.* **2017**, *3*, e1602165.

[19] G. A. Sewvandi, K. Kodera, H. Ma, S. Nakanishi, Q. Feng, *Sci. Rep.* **2016**, *6*, 30680.

[20] B. Chen, X. Zheng, M. Yang, Y. Zhou, S. Kundu, J. Shi, K. Zhu, S. Priya, *Nano Energy* **2015**, *13*, 582.

[21] T. Leonhard, A. D. Schulz, H. Röhm, S. Wagner, F. J. Altermann, W. Rheinheimer, M. J. Hoffmann, A. Colsmann, *Energy Technol.*, https://doi.org/10.1002/ente.201800989.

[22] A. Pockett, G. E. Eperon, T. Peltola, H. J. Snaith, A. Walker, L. M. Peter, P. J. Cameron, *J. Phys. Chem. C* **2015**, *119*, 3456.

[23] S. Ravishankar, C. Aranda, P. P. Boix, J. A. Anta, J. Bisquert, G. Garcia-Belmonte, *J. Phys. Chem. Lett.* **2018**, *9*, 3099.

[24] G. Sharada, P. Mahale, B. P. Kore, S. Mukherjee, M. S. Pavan, C. De, S. Ghara, A. Sundaresan, A. Pandey, T. N. Guru Row, D. D. Sarma, *J. Phys. Chem. Lett.* **2016**, *7*, 2412.

[25] H. Yan, F. Inam, G. Viola, H. Ning, H. Zhang, Q. Jiang, T. Zeng, Z. Gao, M. K. Reece, *J. Adv. Dielectr.* **2011**, *01*, 107.

[26] B. Jaffe, W. R. Cook Jr., H. Jaffe, *Piezoelectric Ceramics*, Academic Press, London, New York **1971**.

[27] J. Fousek, *J. Appl. Phys.* **1969**, *40*, 135.

[28] P. R. Potnis, N.-T. Tsou, J. E. Huber, *Materials* **2011**, *4*, 417.

[29] T. Hatanaka, A. Sawada, *Jpn. J. Appl. Phys.* **1989**, *28*, L794.

[30] A. Poglitsch, D. Weber, *J. Chem. Phys.* **1987**, *87*, 6373.

[31] Y. Dang, Y. Liu, Y. Sun, D. Yuan, X. Liu, W. Lu, G. Liu, H. Xia, X. Tao, *CrystEngComm* **2015**, *17*, 665.

[32] J.-P. Yang, M. Meissner, T. Yamaguchi, X.-Y. Zhang, T. Ueba, L.-W. Cheng, S. Ideta, K. Tanaka, X.-H. Zeng, N. Ueno, S. Kera, *Sol. RRL* **2018**, *2*, 1800132.

[33] Y. Yuan, Q. Wang, Y. Shao, H. Lu, T. Li, A. Gruverman, J. Huang, *Adv. Energy Mater.* **2016**, *6*, 1501803.

[34] P. Würfel, P. Batra, *Ferroelectrics* **1976**, *12*, 55.

[35] Y. Liu, L. Collins, A. Belianinov, S. M. Neumayer, A. V. Ievlev, M. Ashmadi, K. Xiao, S. T. Retterer, S. Jesse, S. V. Kalinin, B. Hu, O. S. Ovchinnikova, *Appl. Phys. Lett.* **2018**, *113*, 072102.

[36] Q. N. Chen, Y. Ou, F. Ma, J. Li, *Appl. Phys. Lett.* **2014**, *104*, 242907.

[37] J. Li, J.-F. Li, Q. Yu, Q. N. Chen, S. Xie, *J. Materiomics* **2015**, *1*, 3.

[38] P. Würfel, I. P. Batra, J. T. Jacobs, *Phys. Rev. Lett.* **1973**, *30*, 1218.

[39] H. Irie, *J. Appl. Phys.* **2001**, *90*, 4089.

[40] P. Ganesh, E. Cockayne, M. Ahart, R. E. Cohen, B. Burton, R. J. Hemley, Y. Ren, W. Yang, Z.-G. Ye, *Phys. Rev. B* **2010**, *81*, 144102.

[41] J. M. Frost, K. T. Butler, A. Walsh, *APL Mater.* **2014**, *2*, 081506.

[42] N. P. Gallop, O. Selig, G. Giubertoni, H. J. Bakker, Y. L. A. Rezus, J. M. Frost, T. L. C. Jansen, R. Lovrincic, A. A. Bakulin, *J. Phys. Chem. Lett.* **2018**, *9*, 5987.

[43] L. Z. Tan, F. Zheng, A. M. Rappe, *ACS Energy Lett.* **2017**, *2*, 937.

[44] D. Rossi, A. Pecchia, M. Auf der Maur, T. Leonhard, H. Röhm, M. J. Hoffmann, A. Colsmann, A. Di Carlo, *Nano Energy* **2018**, *48*, 20.

[45] Y. Yuan, P. Sharma, Z. Xiao, S. Poddar, A. Gruverman, S. Ducharme, J. Huang, *Energy Environ. Sci.* **2012**, *5*, 8558.

[46] S. Ravishankar, C. Aranda, P. P. Boix, J. A. Anta, J. Bisquert, G. Gcarcia-Belmonte, *J. Phys. Chem. Lett.* **2018**, *9*, 3099.